Published in Solar Energy Materials and Solar Cells 66, issue 1-4, 397-403, 2001
which should be used for any reference to this work

Microcrystalline n-i-p solar cells deposited at 10 Å/s by VHF-GD

L. Feitknecht[a,*], O. Kluth[b], Y. Ziegler[a], X. Niquille[a], P. Torres[a], J. Meier[a], N. Wyrsch[a], A. Shah[a]

[a]*Institute of Microtechnology (IMT), rue A.-L. Breguet 2, CH-2000 Neuchâtel, Switzerland*
[b]*Institute of Thin Film and Ion Technology, Forschungszentrum Jülich (FZJ), D52425 Jülich, Germany*

Abstract

In the present paper, we report on thin-film microcrystalline silicon solar cells grown at high deposition rates on back-reflectors with optimised light-scattering capabilities. A single-junction solar cell with a conversion efficiency of $\eta = 7.8\%$ (2 μm thickness) was fabricated at a deposition rate of 7.4 Å/s. Another microcrystalline cell was successfully implemented in a "micromorph" tandem (i.e. a microcrystalline/amorphous tandem cell with n–i–p–n–i–p configuration); the resulting initial conversion efficiency was $\eta = 11.2\%$. A 4 μm thick single-junction cell at a deposition rate of 10 Å/s and with a conversion efficiency of $\eta = 6.9\%$ was fabricated on a non-optimised substrate. Special attention is drawn to near-infrared spectral response and interface optimisation.

Keywords: Microcrystalline silicon; High deposition rate; Thin-film n-i-p solar cell; VHF-GD

1. Introduction

Hydrogenated microcrystalline silicon (μc-Si:H) thin-film solar cells can be deposited with substantial advantages by using the VHF-GD (very high frequency-glow discharge) method: high deposition rates are feasible, damage due to ion bombardment is minimised, CPM defect densities are low and solar cell performances excellent [1]. In the past the Neuchâtel group had mainly concentrated on the glass-p–i–n (superstrate) cell configuration. In the superstrate configuration, single-junction p-i-n

* Corresponding author. Tel.: + 41 32 718 33 62; fax: + 41-32-718-32-01.
E-mail address: luc.feitknecht@imt.unine.ch (L. Feitknecht).

devices, as well as "micromorph" p–i–n–p–i–n tandem cells (consisting of a microcrystalline bottom and an amorphous top cell) had been fabricated, showing encouraging results (over 8% stabilised efficiency for single junction and over 11% stabilised efficiency for tandem cells [2]).

The Neuchâtel (IMT) and Jülich (FZJ) research groups have recently also investigated the n-i-p (i.e. the "inverted" or "substrate") configuration, since this cell structure has some interesting advantages [3]: Temperatures up to 400°C can be considered here for deposition of the ⟨i⟩ absorber layers, since the temperature-sensitive ⟨p⟩ layer is deposited at the end of the process at a possibly much lower temperature. Moreover, in addition to transparent substrates (e.g. glass as usable in the superstrate configuration), a variety of opaque substrates like metals and plastics can also be used here.

Total production time finally depends both on the deposition rate and on the cell thickness. Thus, the motivation of this work is to increase not merely the deposition rates [4], but also to realise efficient and thin microcrystalline solar cells on back-reflectors with optimised light-trapping properties. In fact, the optical path-length in the solar cell can be increased with a high light-scattering capability of the substrate, and the longer the path-length of photons through the cell is, the higher the absorption probability of light in the cell becomes.

2. Experimental

μc-Si:H silicon n-i-p solar cells and intrinsic absorber films were both deposited in a single-chamber VHF-GD reactor at plasma excitation frequencies between 70 and 130 MHz. Typical deposition parameters for the intrinsic layer are: base pressure of the vacuum chamber $p_{\text{base}} < 4 \times 10^{-8}$ mbar, deposition pressure $p = 0.1 - 0.9$ mbar, applied plasma power $P = 5 - 30$ W, substrate temperature around 200°C. A gas purifier was used to avoid incorporation of detrimental oxygen contamination [5]. These conditions lead to deposition rates in the range of 8–10 Å/s. Amorphous silicon top cells were deposited in another, comparable single-chamber VHF-GD deposition system [6].

The intrinsic μc-Si:H films used for material characterisation were deposited on sodium-free AF45 glass substrates from Schott and have thicknesses between 2.0 and 2.4 μm. A series of films deposited with silane concentrations, $SiH_4/(SiH_4 + H_2)$, ranging from 5 to 8% was characterised. Surface profiling was performed with a Burleigh Vista 100 atomic force microscope (AFM) in contact mode. Further characterisations of these films (dark conductivity measurements, σ_{photo}, SPV, SSPG and the ambipolar diffusion length L_{amb}) are to be published elsewhere [7,8].

The substrates for solar cells (glass/Ag/ZnO or stainless steel/Ag/ZnO stack combined with a post-deposition chemical-etching of the sputtered ZnO with diluted HCl) were prepared at FZJ [9]. Optical measurements on all substrates were performed on a double beam (Perkin Elmer L900 with integration sphere) spectrometer in the range of 350–1200 nm. Special interest was drawn to both, the diffuse and the total reflectance. Current vs. voltage characterisation was performed under AM1.5 conditions at

100 mW/cm^2, using a two-source solar simulator. The short-circuit current densities (J_{SC}) were calibrated by integrating the product of spectral response (SR) data in the range of 350–1000 nm times the AM1.5 sun spectrum.

3. Results and discussion

3.1. μc-Si:H silicon material and n–i–p solar cells

As shown in Fig. 1b, one observes a pronounced rise of the deposition rate as one increases silane concentration and approaches the microcrystalline/amorphous transition zone. A second effect (shown in Fig. 1a) is a strong variation in the surface roughness of the μc-Si:H silicon films [10]: In fact, one way to quantify the light trapping (besides performing optical absorption measurements) is to analyse the surface roughness of the μc-Si:H ⟨i⟩-film by means of surface profiling. By scanning an area of $2 \times 2\,\mu m$ with the AFM, we obtained the surface roughness expressed by the root mean square (rms) value. With increased silane concentration, the rms value of the surface roughness rises to a maximum of 37 nm, then falls down to 4.7 nm. This

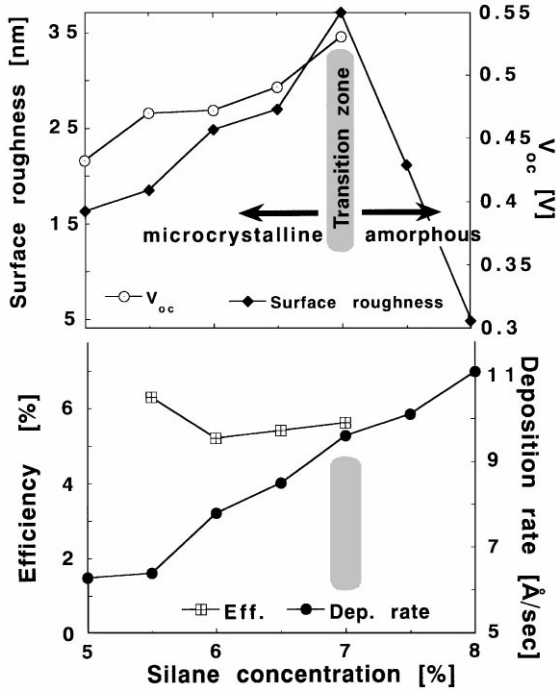

Fig. 1. (top): Surface roughness (from AFM scans), open circuit voltage V_{OC}, cell efficiency and (bottom) deposition rate in function of silane to total gas concentration in the VHF-plasma. Note the morphological transition from μc-Si:H silicon to amorphous silicon at a silane concentration of 7%.

zone of sudden change from a highly textured surface to a nearly untextured surface may be identified as a part of the transition zone from microcrystalline to amorphous morphology; there is probably still a substantial amount of crystalline volume fraction present in the film. Note that a rough surface texture of the silicon films leads to an enhanced apparent absorption, and therefore an increase in spectral response can be expected.

We further observed that V_{OC} can be increased up to 531 mV by using higher silane concentrations. However, a further optimisation of the fill factor and of J_{SC} is yet necessary for these high-V_{OC}-cells. We should also try to achieve a better light scattering of the substrate and better light trapping of the cell material in order to remedy for the present low value of J_{SC}.

3.2. Comparison of J_{SC} of n-side with p-side illuminated cells

In order to compare the critical interfaces right at the beginning of the cell-deposition process (where crystallite nucleation has to take place), we performed the spectral response (SR) measurement on both sides of the cell (i.e. bifacially): the SR obtained by conventional p-side illumination was compared with an 'unusual' SR measurement through a transparent substrate and through the n-side of the solar cell (see Fig. 2). This allows an identification of absorption/collection problems in the short wavelength region, since this blue part of the spectrum never reaches the back-reflector when executing the conventional illumination process of a 2–3 μm thick cell. The ratio of the two J_{SC} generated through the n-side and the p-side gives a symmetry factor (f_{np}), which should approach 100% in the ideal case of symmetry (of course, ignoring differences in mobility and lifetime of electrons and holes). This method allows for an analysis of the solar cell on transparent substrates; the latter can, however, be considered to be roughly comparable to the optimised back-reflector substrates used otherwise.

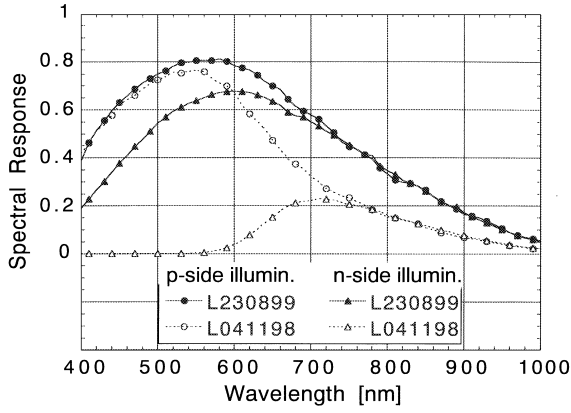

Fig. 2. Spectral response on two μc-Si:H silicon cells before and after interface optimisation. p-side illumination (left) generates an J_{SC} of 14.3 and 19 mA/cm^2 , respectively, whereas n-side illumination (right) generates an J_{SC} of 3.4 mA/cm^2 before and 16.1 mA/cm^2 after interface optimisation.

First cells had a symmetry factor of only 24%. An increase of this value to 85% was possible due to n–i interface optimisation. The later cells with $f_{np} = 85\%$ have a much better overall performance than the cells with a $f_{np} < 57\%$, especially in the near-IR region (J_{SC} of 24 mA/cm^2). Such high short-circuit currents of μc-Si:H silicon n–i–p cells can be explained by a successful combination of a good light trapping and an enhanced light-scattering capability of the back-reflector.

3.3. Light-scattering capability of back-reflectors

Fig. 3 shows the reflectance measurement of an optimised back-reflector which is used as substrate for n–i–p solar cells. Note that the curves for total reflectance and for diffuse reflectance follow each other very closely in the near-IR zone (around 1000 nm). This means that, in the near-IR zone, 70% of the reflectance is diffuse and just 10% is specular reflectance.

The quality of the back-reflectors can be evaluated with the help of optical measurements (e.g. with a spectrometer), but also by determining the overall performance of the solar cell. A series of four substrates of different surface texture were fabricated and incorporated into micromorph n–i–p–n–i–p solar cells. The surfaces of the substrates (glass/Ag/ZnO stacks) were textured in a chemical etch during 4, 7, 15 and 30 s, respectively. Note that "no etch" means a flat surface, and the longer the etch time the higher the surface texture of the substrate becomes.

The μc-Si:H silicon bottom cells were deposited in two runs on four substrates of different surface textures. Table 1 shows the dependency of J_{SC} and of substrate texture in the two series we have analysed. A maximum J_{SC} is generated on the back-reflector when the latter was etched during 7 s. There is no significant influence of texturing on the top cell current. In consequence of that observation, further substrates were fabricated with a surface texturation etch time in the range of 7–15 s. Fig. 4 shows the best n–i–p cell with better near-IR response due to optimised interfaces and highly scattering back-reflector, grown at 7.4 Å/s ($J_{SC} = 24\,\text{mA/cm}^2$, $V_{OC} = 462\,\text{mV}$, FF = 70%, $\eta = 7.8\%$).

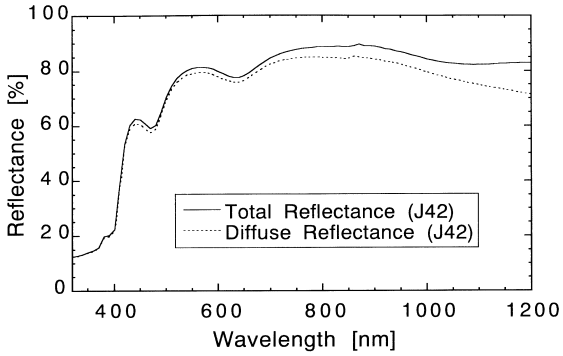

Fig. 3. Diffuse and total reflectance of an enhanced back-reflector (steel/Ag/ZnO) as used as solar cell substrate. Note the high diffuse part of 70% in the near-IR spectral region.

Table 1
Influence of using different surface-textured substrates, on the J_{SC} values of micromorph n-i-p-n-i-p cells. The substrates are etched during an etch time that varies between 4 and 30 s. Note that the tandems of run 1 are all bottom-cell limited. The optimum etch time for this case is around 7 s. A further support of this is given by run 2, where only the current-limiting cell is reported

Etch time:	4 s	7 s	15 s	30 s
	Bottom/top	Bottom/top	Bottom/top	Bottom/top
J_{SC} run 1 (mA/cm^2)	7.3/10.5	9.25/10.8	8.1/10.5	7.2/10.7
J_{SC} run 2 (mA/cm^2)	4.5	7.3	6.6	6.2

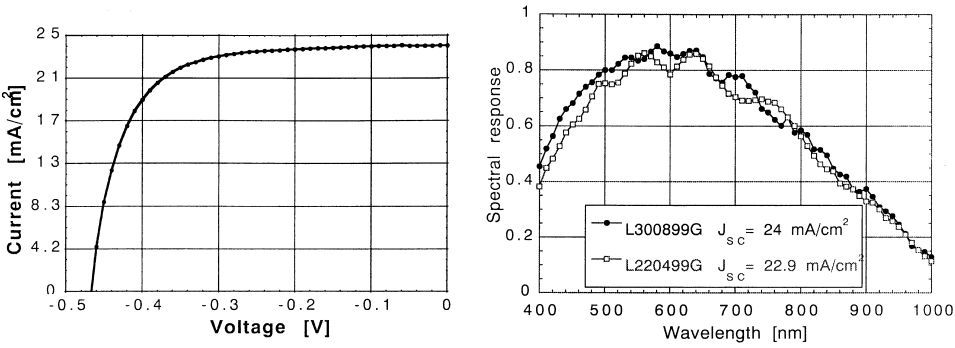

Fig. 4. *I–V* curve (left) and spectral response (right) of the so far best single-junction microcrystalline n–i–p cells of 7.8% conversion efficiency, 2 μm thickness; this cell was grown at 7.4 Å/s with optimised interfaces, on a highly light-scattering substrate.

3.4. Micromorph n–i–p–n–i–p solar cells

The so far best micromorph tandem had 11.2% initial efficiency ($V_{OC} = 1.4$ V, FF = 71%, $J_{SC} = 11.3$ mA/cm^2) but was fabricated with a not yet optimised bottom cell with near-IR absorption properties clearly inferior to those shown for the optimised single-junction cell in Fig. 4. Light-soaking experiments of that micromorph solar cell showed a relative degradation of 13% after 1152 h, while the high-V_{OC} microcrystalline single-junction solar cell remains stable. Thus, there is room for further improvement.

4. Conclusions

High deposition rates as well as a reduced bottom cell thickness are mandatory to enable future industrialisation of the micromorph tandem cell: In fact, both these points strongly influence the production time of micromorph modules. In this work we present a 2 μm thin microcrystalline n-i-p cell (conversion efficiency of $\eta = 7.8\%$)

which was fabricated at a deposition rate of 7.4 Å/s. The successful combination of optimised substrates and high deposition rate solar cells has so far led to conversion efficiencies of 11.2% (initial) for the micromorph tandem configuration.

The use of higher deposition rates (up to 10 Å/s) does not seem to be a limiting factor in achieving high efficiencies (single-junction efficiencies around $\eta = 7\%$). On the other hand; A key issue to obtain even more efficient micromorph solar cells will be the increase of V_{OC} in the microcrystalline bottom cell; Whilst still maintaining high values of J_{SC} and FF.

Bifacial solar cell illumination through the n-side and p-side was used as a tool to optimise interfaces i.e. to improve the growth process right at the initial stage of cell deposition. Thereby, an increase of the symmetry factor f_{np} (equal to the ratio of short circuit currents n-J_{SC} /p- J_{SC} when illuminated from the n-side and the p-side) from 24 to 85% was obtained (resulting in nearly symmetric spectral response through n- and p-side).

Acknowledgements

This work has been carried out within the European project NEST under Contract JOR3-CT97-0145. The IMT acknowledges financial assistance by the Swiss government through the Swiss Federal Office for Education and Science under contract 96.0340. FZJ acknowledges financial support from the E.U. and from the German Federal Ministry of Education and Research.

References

[1] P. Torres, Ph.D. Thesis Uni Neuchâtel, ISBN 3-930803-51-8, UFO Konstanz (D) 1999, www.ufo.znet.de.
[2] J. Meier, H. Keppner, S. Dubail, U. Kroll, P. Torres, P. Ziegler, J.A. Anna Selvan, J Cuperus, D. Fischer, A. Shah, Mat. Res. Soc. Symp. Proc. Vol. 507, p. 139.
[3] N. Wyrsch, P. Torres, M. Goetz, S. Dubail, L. Feitknecht, J. Cuperus, A. Shah, B. Rech, O. Kluth, S. Wieder, O. Vetterl, H. Stiebig, C. Beneking, H. Wagner, Proceedings of 2nd WCPEC (Vienna 1998) p. 467.
[4] P. Torres, J. Meier, U. Kroll, N. Beck, H. Keppner, A. Shah, Proceedings of 26th PVSC (Anaheim, 1997) p. 711–714.
[5] P. Torres, J. Meier, R. Flückiger, U. Kroll, J.A. Anna Selvan, H. Keppner, A. Shah, S.D. Littelwood, I.E. Kelly, P. Giannoulès, Appl. Phys. Lett. 69 (10) (1996) 1373.
[6] P. Pernet, M. Goetz, H. Keppner, A. Shah, Mat. Res. Soc. Symp. Proc. Vol. 452, pp. 889–894.
[7] C. Droz, M. Goerlitzer, N. Wyrsch, A. Shah, J. Non-Cryst. Solids 266–269 (2000) 319–324.
[8] N. Wyrsch, L. Feitknecht, C. Droz, P. Torres, A. Shah, A. Poruba, M. Vanecek, J. Non-Cryst. Solids 266–269 (2000) 1099–1103.
[9] O. Kluth, O. Vetterl, R. Carius, F. Finger, S. Wieder, B. Rech, H. Wagner, Mat. Res. Soc. Symp. Proc. Vol. 557, p. 731.
[10] E. Vallat-Sauvain, U. Kroll, J. Meier, N. Wyrsch, A. Shah, J. Non-Cryst Solids 266–269 (2000) 125–130.